[1]K Saravanan

[2]Dr. M. Rajesh Khanna

[3]U. Arul

[4]Dr. S M Padmaja

[5]Lakshmana Phaneendra Maguluri

[6]Dr. B. Varaprasad Rao

[7]Dr. Kireet Muppavaram

Improved Adaptive Network-Based Fuzzy Inference System Approach for Power Flow Analysis in Interconnected DC Microgrid

Journal of Electrical Systems

Abstract: - High-performance power conversion needs are becoming more and more important for microgrid applications. In actuality, many contemporary DC distribution systems use isolated bidirectional dc-dc converters. Hence, in this paper, an Improved Adaptive Network-based Fuzzy Inference System (IANFIS)is developed to control the output power of the components and reduce the variation among the consumption and generation of the power while managing a constant DC bus voltage. This work proposes a power management control strategy that ensures the power balance of a stand-alone DC microgrid where DAB converters link the battery energy storage (BES) unit and the renewable energy source (RES). The generation side, or photovoltaic (PV) system and BES, is coupled to the storage systems and renewable energy sources. Furthermore, a DC microgrid is connected to the load demand. The load demand is compensated with the help of the storage and generation systems with the help of a dual active bridge converter. The DAB is connected with the dual DC microgrid system for managing power flow among the two DC microgrids. This dual active bridge converter is utilized to balance the power among Dual DC microgrids. The proposed methodology is developed to manage the power among generation and load demand management. The proposed method is evaluated on a dual active bridge converter connected microgrid system with the components of PV and BESS respectively.

Keywords: interconnected DC microgrid, improved adaptive network-based fuzzy interference system, battery energy storage system, Dingo optimizer, and dual DC microgrid

[1] [1]Associate Professor, Department of Information Technology, R.M.K Engineering College, Kavaraipettai, Tamil Nadu, India

ksn.it@rmkec.ac.in

[2]Associate Professor, Department of INFORMATION TECHNOLOGY, VEL TECH MULTI TECH DR. RANGARAJAN DR. SAKUNTHALA ENGINEERING COLLEGE, AVADI, CHENNAI, Tamilnadu rajeshkhanna@veltechmultitech.org

[3]Professor, Department of Computer Science and Engineering, Saveetha School of Engineering, Saveetha Institute of Medical and Technical Sciences (SIMATS), Saveetha University, Chennai, Tamil Nadu, India

arulmee08@gmail.com

[4]Professor, Department of Electrical and Eletronics Engineering,Shri Vishnu Engineering College for Women, Vishnupur, Bhimavaram, Andhra Pradesh, India.

padmaja_vvr@yahoo.com

[5]Associate Professor, Department of Computer Science and Engineering, Koneru Lakshmaiah Education Foundation, Green Fields, Vaddeswaram, Guntur Dist., Andhra Pradesh - 522302, India

phanendra51@gmail.com

[6]Professor, Department of Computer Science and Engineering,RVR&JC College of Engineering, Guntur, AP.

bvpr@rvrjc.ac.in

[7]Assistant Professor, Dept of CSE, GITAM DEEMED To be University, Hyderabad

kmuppava@gitam.edu

Copyright © JES 2024 on-line : journal.esrgroups.org

1. Introduction

Recently, the inseparable sections of power systems have been called microgrids which comprise different interconnected electrical loads and distributed generations (DGs) in which the grid-connected mode or islanded mode is operated [1]. Efficiency, power losses, and dependability are three significant benefits offered to today's power systems, and microgrids are devoted to solving the majority of the studied issues in the contemporary power system.

[2].Microgrids, for example, offer the possibility of providing a few of the electrical requirements through emergencies that will restore system performance by increasing power quality and reliability [3]. Another advantage of these processes is an excellent choice for generating power to remote locations far off the primary electricity network in which the electric grid doesn't occur. This will be noted the microgrids are categorized into 3 major types: AC, DC, and both AC-DC microgrids.

Even though aforementioned, all Converter and electrical equipment in the AC microgrids have been associated with a single AC bus. In these kinds of processes, the same existence of power units and DC loads is unavoidable [4]. These DC units are connected to the AC microgrids of AC buses by a variety of devices, including DC2AC inverters and AC2DC rectifiers. The DC bus link connects the power units and AC loads via an AC2DC rectifier it must be mentioned that now in DC microgrids [5]. Many equipment, such as DC2AC inverters and AC2DC rectifiers, link these DC units to the AC microgrids of AC buses. Inside the sense of a classical power grid, the OPF issue is traditionally addressed using centrally controlled methodologies just at the transmission grid level.

The OPF issue would either be overlooked or evaluated in the distribution network. With the deeper interdependence of DERs and DR, as well as the continuing liberalization of the electricity market, the centralized method faced different challenges such as (i) the percentage of generating units and users growing dramatically; (ii) the distribution grid must be factored appropriately [6]. The scale of the OPF issue is typically too big to also be fixed and centralized due to the immense number of branches and nodes. As a result, far more effort has gone into integrating multiple algorithms again for the OPF issue [7]. In power systems, the existing researchers did not discuss or focus on hybrid microgrid optimization but they failed to consider other aspects such as energy transactions and cyber-security of data enhancement, etc.

No current research has determined the power of solar panels and wind units based on stochastic factors, such as hybrid stochastic AC-DC microgrids [8].To enhance energy transaction and data transmission security layer enhancement, optimal management and secure enhancement were introduced and investigated. Recent studies presented several control techniques to overcome these challenges. From this analysis, the coupledterms are neglected as well as the nonrotational structure is described, which is low cost and simple [9]. The proportional-resonant (PR) compensators and sub-grid utilize the proportional-integral (PI) compensators. The first control layer is initialized to rectify the error. The upstream power grid with the whole sub-grid synchronization aims at the tertiary layer. The power fluctuation amplitude is changed by implementing the adjustable scalar [10]. The sophisticated scheme removes and determines the oscillating power with its negative and positive components.

The article is organized the rest as follows: The relevant work analysis of the connected DC microgrid with power flow management is given in Section 2. A detailed explanation of the suggested methodology is provided in Section 3. Section 4 explains the results and assessment of the suggested method. In section 5, the paper's summary is provided.

2. Literature Review

Based on microgrid technology considering uncertainty, Li et al. [11] suggested the security improvement of interconnected hybrid AC-DC microgrids. There are fewer power electronics connections needed to convert DC to AC electricity because this is far more economical than traditional grids. But there are numerous benefits to a scheme, also there are numerous drawbacks. For example, power consumption of the system is much more difficult from a complete system point of view because any adjustments in every subsystem can impact the electricity control of the project scheme. Employ the copula model to create the stochastic load flow and realistic model. Efficiently, the data is saved via cloud computing to store more data.

In grid-connected hybrid microgrids, the modified UIPC with interconnected AC–DC microgrids power flow control was designed by Zolfaghari et al. [12]. Link the DC buses and the main grid through the LPC connects the AC microgrid in which the inductance mode (IM) or capacitance modes (CM) are operated. Inmembership functions design, the errors were reduced and the H filtering method optimizes the fuzzy inference system. The DC microgrid uses a BPC to supply the DC voltage needed for LPCs. Variably adjust the DC-link voltage LPCs, and the PV system supplies the DC microgrid voltage. Depending upon robust multiple-surface sliding mode control, the DC link fluctuations are stabilized. For hybrid microgrids, the proven power flow control strategy shows superior outputs based on the simulation results.

The negotiation with multiple interconnected microgrids of decentralized cooperative optimal power flow was analyzed by Li et al. [13]. Initially, formulate the coupled microgrids and standalone microgrids. The coupled OPF problem was solved via a decentralized approach. The negotiation between microgrids was led with the pled OPF problem of the optimal solution in which local OPF problems were solved with the help of each microgrid. Share the information among the microgrid and preserve each microgrid's privacy. This model produced better optimality gap results when compared to the AC OPF and the DC OPF.

In hybrid microgrids, the UIPC interconnects multiple AC and DC microgrid clusters of power exchange control were introduced by Zolfaghari et al. [14]. The microgrid clusters are linked together by the UIPC which also allows for power transfer among clusters. For UIPC control, a requirement to achieve the desired fractional order-based control concept can be defined. Numerical models are presented for exchange controllability between clusters of DC and AC microgrids and with the main grid.

Panda et al. [15] developed an effective SoC-balancing-based power management model for DC microgrids with interconnected sub-grids. Create a state transition technique that is DC signaling-oriented for coordinating generation and storage. Presenting the SoC-based IBC secondary control model, which is based on power-sharing between subgrids through SoC balancing. The low-SoC battery is quickly charged, and deep discharge of the battery is avoided. During a fault scenario, guarantee the transient stability without the need for any extra mode detection models. A supplementary IBC controller was used to restore distributed power-sharing while limiting information transmission through low bandwidth communication (LBC). IBC controllers enhanced battery performance and made efficient use of PV generations. The viability of this model is verified by MATLAB simulation based on the OPAL-RT real-time digital simulator; nevertheless, the computational complexity is increased.

3. Proposed System Model

Normally, the interconnected DC microgrid system with a utility system with the consideration of AC/DC conversion phases. Thus, figure 1 shows the entire structure of the suggested system. The purpose of this suggested system is to enhance the power balance of a DC microgrid through the construction of a power management control system that can operate independently. PV and a battery energy storage system are included in the design of the suggested system.

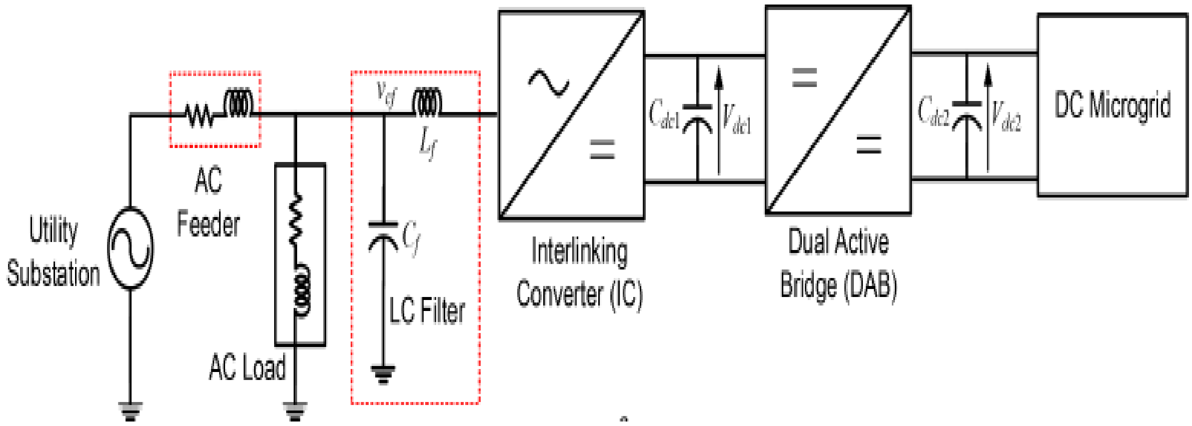

Figure 1: block diagram of the proposed methodology

PV and BES are used in the construction of the suggested DC microgrid system. Since the PV system is susceptible to external factors, the maximum power point tracking controller is managed by the boost converter. By modifying the duty cycle to attain the desired output voltage, the boost converter is employed to increase the necessary voltage. The transformer-less three-phase, three-leg VSC is the definition of an interconnected converter [16]. Subsequently, the DAB is linked to the connecting converter's DC link. Both the LC filter and reduced converter loss resistance are used to lessen high-frequency oscillation. In the part that follows, the modeling of the PV system and DAB with controller is described.

3.1. Modelling of PV system

The section provides a standard mathematical analysis of photovoltaic cells, which can be quantified as electrical apparatuses that produce electricity from solar radiation depending on the degree of irradiance. Solar radiation is captured through the use of PV panels, which are referred to as sustainable energy sources. The PV panel can be constructed to use semiconductor panels, which are capable of producing atoms based on differences in behavior by absorbing photons of sunshine and emitting electrons. Based on the behavior of atoms, current flow can be processed to generate power that is used in a variety of ways. The MPPT controller needs to be built to maximize PV power extraction while avoiding environmental behavior issues. Figure 2 displays the PV system's general model. To supply leakage current and internal resistance, which promote current flow in PV panels, parallel resistors, photocurrent, and diodes with equivalent circuit models are built [17].

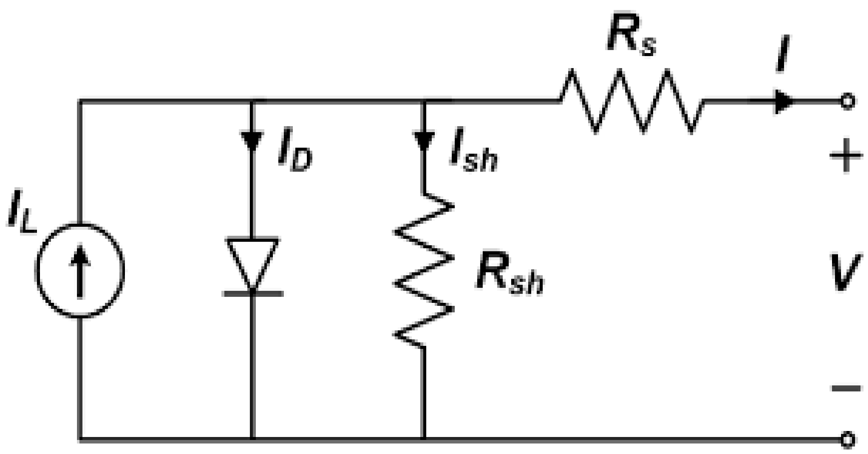

Figure 2: Equivalent circuit model of PV system

r cell's current plus voltage cabe expressed as follows:

$$I_C^{PV} = \frac{I_{ph}}{1-C^{-d}}\left[exp^{\frac{voc}{a}}\left(\frac{qv+qr_vI}{NKT}\right)-1\right]-\frac{V+R_sI}{R_{sh}} \quad (1)$$

Here, I^{ph} can be described as is the electric current of PV.

The current of PV panel can be defined as$I$, $q = (1.6 * 10^{-19}C)$ can be considered as electron charge.

T can be considered as temperature of each cell in PV panel.

N can be defined as ideal factor of PV.

Shunt resistance can be described asR_{sh}.

Series resistance can be described asR_s.

Open circuit voltage can be described asV_{oc}.

The controllers and PV panels are developed in response to variations in irradiation. The different irradiance levels in each solar panel are taken into account to compile a database. Variations in the level of irradiance create changes in the output power of the solar panel. With the converter, the correct generation of control signals is maintained in a constant irradiance. The MPPT controller modifies the recommended converter duty cycle (D) to maintain the PV panel at its designated working points, which are usually at maximum power point. In this case, a projected MPPT-based controller with input-based regulation of the converter duty cycle can be built.

3.1. Dual Active Bridge Converter

The purpose of the suggested enhanced converter is to control power flow from the utility grid to the DC microgrid. Figure 3 depicts the suggested converter.

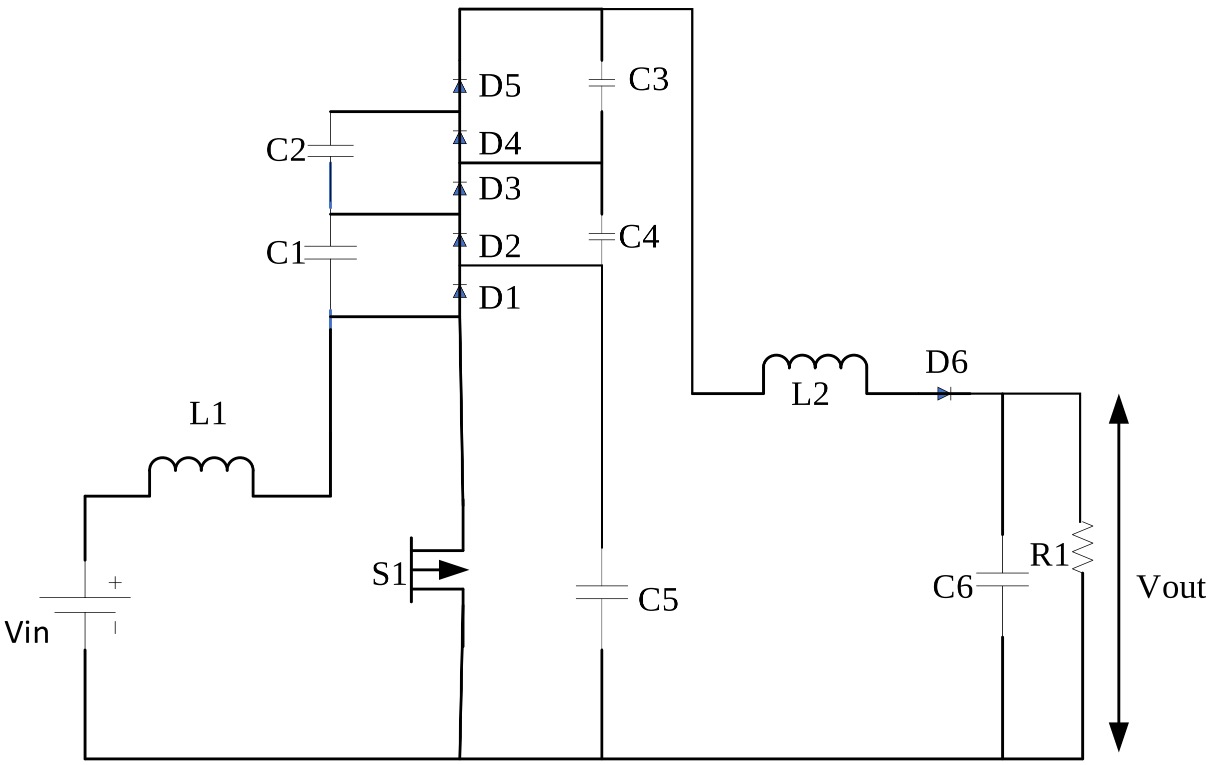

Figure.3: Design of proposed converter

The following are some of the unique features of this proposed converter:

- The semiconductor device is regarded as high
- The capacitor spent has a high stowage voltage in addition to being understood to be perpetual
- This proposed converter operates in a stable mode of continuous conduction.

The key switch S1, inductor coils L1 and L2, diodes D1–D6, capacitors C1–C6, and key switch D1 make up the suggested model [18]. Voltage Tripler (VT) loop can be attached in order to increase the static voltage ratio in the suggested converter. There are two ways of operation for the suggested converter. Figure 4 displays the proposed converter's mode of operation.

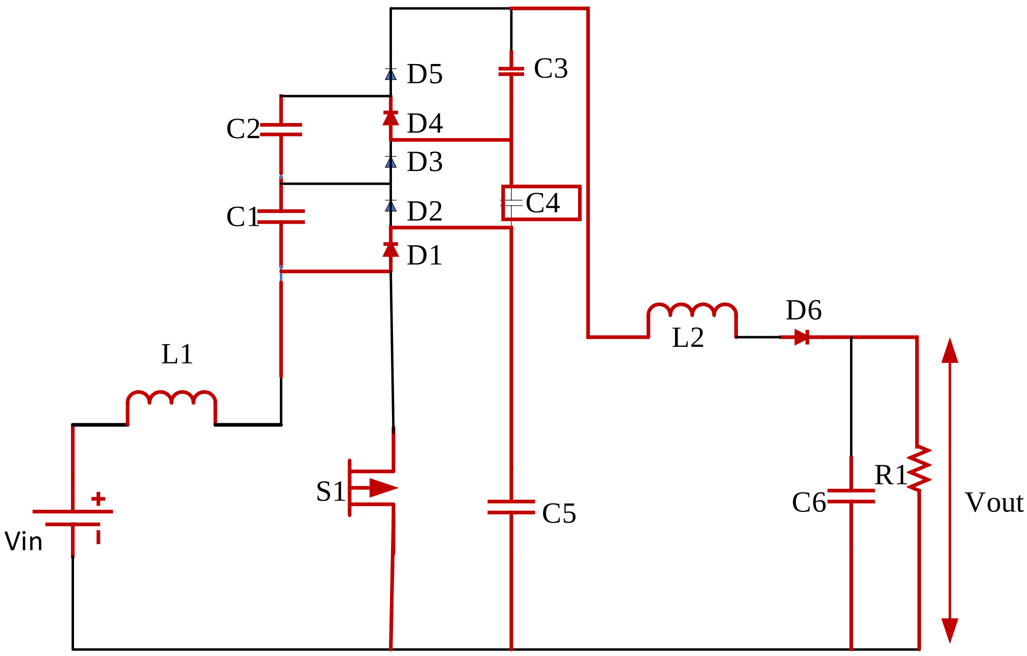

(a)

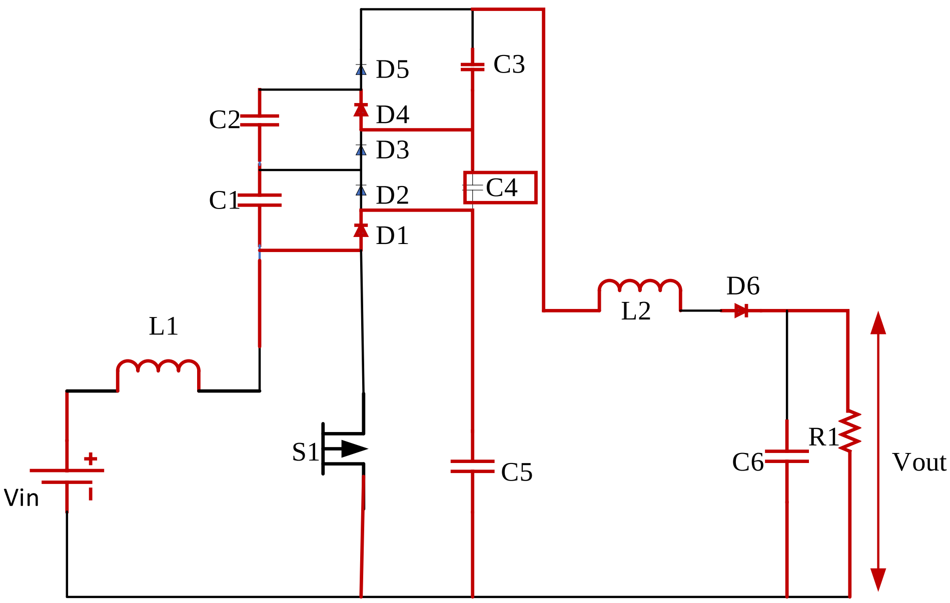

(b)

Figure.4: Proposed DC-DC converter operation (a) mode 1 and (b) mode 2

Mode 1:

The switch (S1) is closed in this mode. D1, D3, and D5 diodes exhibit opposite bias. Furthermore, the diodes D6, D4, and D2 are shown as being in the ON state. L1 receives the input voltage source (Vin), while L2 receives the distribution of voltages Vc1–Vc2-Vc3. It is possible to store the inductor energy in this process mode. In order for the DC-DC converter to function, the capacitor of C6 is forward to the load. This mode is finished based on the switch (S1) being opened. In a similar vein, at T=T1, the D3 and D1 currents reach zero.

Mode 2:

The diodes (D4, D2) are regarded as being in an open condition in this process mode, which allows the switch (S1) to be opened. The forward directions are connected to the diodes of D5, D3, and D1. The capacitors are charged by means of the L2 and L1 inductors. Energy can be transferred to the load situation at the end of the mode. While the primary source is in ON status, this process continues. This set is being continued with the next set. The converter output, which is calculated as follows, is equal to the total of the three-level capacitor source.

$$Vc6 = Vc3 + Vc4 + Vc5 \tag{2}$$

In the normal state, the inductor value can be described as zero. Based on that, the static gain is calculated follows,

$$VinD = (Vc5 - 3Vin)(1 - D) \tag{3}$$

Where,Vincan be described as input voltage and Dcan be described as duty cycle. Based on above equation, the $Vc5$can be computed below,

$$Vc5 = \frac{3Vin}{1-D} \tag{4}$$

In the stable state condition, the inductor$L2$is zero voltage which formulated as follows,

$$(Vc5 - Vc1)D = (V0 - Vc5)(1 - D) \tag{5}$$

From the computation of above equation, the$C1$voltage is presented below,

$$Vc5 = V0 - Vc3 - Vc4 - Vc5 \tag{6}$$

From the above equation, the static voltage can be presented below,

$$\frac{V0}{3Vin} = \frac{(1+D)}{(1-D)} \tag{7}$$

From the above equation, the duty cycle can be computed based on below equation,

$$D = \left(1 - \frac{3Vin}{V0}\right) \tag{8}$$

From the capacitor$Cs$and diodes, the switch voltage$Vs$is computed,

$$Vs = \frac{30}{1-0.775} = 133.3V \tag{9}$$

The suggested converter is used to control power flow from the PV system between the DC microgrid and utility grid. The ANFIS controller is the target of the power value error values in the microgrid system. With DO's help, the suggested DC-DC converter's ideal pulses are chosen. The suggested controller balances the load demand in the electric grid and linked MG system, allowing the PV system to operate at its best.

3.2. ANFIS model

The capacity of higher stage reasoning and the low power estimate of the neural network create resilient ANFIS. The integration of the Fuzzy Inference System (FIS) develops the mixed technique known as ANFIS. The Intermediate value among false and true are defined via multi-defined logic called fuzzy logic. Based on the scale consideration, the ranges from low, very low and high can be varied. In a fuzzy reasoning system, form the information base via the number of fuzzy rules namely IF and Then [19].

Initially, the ANFIS passes the input as$R(\vec{x}_1), R(\vec{x}_2), \ldots, R(\vec{x}_n)$. The model of IF and THEN rule is given as follows:

$$R(\vec{x}_1) is U_i, p(\vec{x}_2) is V_i then W_i is$$

$$IFR_i = u_i R(\vec{x}_1) + v_i R(\vec{x}_2) + w_i R(\vec{x}_n) + f_i \tag{10}$$

Where,$R(\vec{x}_1), R(\vec{x}_2), \ldots, R(\vec{x}_n)$ is the input with the fuzzy set areU_i, $V_i$and W_i. Inside the fuzzy region, $OF_i$is the output of fuzzy rules in which the parametersu_i, v_i, w_i and $f_i$are determined during the training process. In the layer-1, each j^{th} node is the square node with its function.

$$OF_{1,i} = \mu_{U_1} R(\vec{x}_1), OF_{1,i} = \mu_{V_1} p(\vec{x}_2), OF_{1,i} = \mu_{W_1} R(\vec{x}_n) \tag{11}$$

From this, the bell-shape selects$\mu_{U_1} p(\vec{x}_1)$,$\mu_{V_1} p(\vec{x}_2)$, $\mu_{W_1} p(\vec{x}_n)$ in which it falls into 1 and 0 intervals for maximum and minimum.

For maximum and minimum, the$\mu_{U_1} p(\vec{x}_1)$,$\mu_{V_1} p(\vec{x}_2)$ and$\mu_{W_1} p(\vec{x}_n)$ are selected via bell-shape that tends to the interval [0, 1].

$$\mu_{U_1} R(\vec{x}_1) = \mu_{V_1} R(\vec{x}_2) = \mu_{V_1} R(\vec{x}_n) = \left(\frac{1}{1+\left(\frac{x-a_i}{b_i}\right)^{2c_i}} \right) \tag{12}$$

Where, $a_i, b_i, c_i$are the parameters in which the outputs the output and incoming signals are multiplied by designing each node in the layer.

$$OF_{2,i} = Yt_i = \mu_{U_i} R(\vec{x}_1) \times \mu_{V_i} R(\vec{x}_2) \times \mu_{Vi} R(\vec{x}_n), i = 1,2 \tag{13}$$

Every node output represents the rule firing strength. The ratio of i^{th} rules firing strength is a sum of eachone rule's firing strengths [20].

$$OF_{3,i} = Yt_i = \frac{Yt_i}{(Yt_1+Yt_2)}, i = 1,2 \tag{14}$$

In the fourth layer, every j^{th} node is the square node and node function.

$$OF_{4,i} = Yt_i S_i, i = 1,2 \tag{6}$$

The parameters in this layer are referenced to via subsequent parameters in the third layer output, isyt_i. The equation that follows represents the total of all incoming signals.

$$OF_{5,i} = \frac{\sum_i Yt_i S_i}{\sum_i Yt_i} \tag{15}$$

Where ω is the predetermined threshold value and this is explained by the following equation [21] which compares the neural network (Z) output.

The below equation compares the neural network (X) result and the predefined threshold valueδ .

$$Re\,s\,ult = \begin{cases} Error, X < \delta \\ NoError, X \geq \delta \end{cases} \tag{16}$$

Find the inaccuracy in the comparison. Every layer estimation limits the fundamentals in the forward channel and transmits input signs. Adjust the ensuing parameters and refresh the error signals in the reverse channel. Based on the ANFIS parameter, the errors are also decreased to identify the improved reliability.

3.3. Dingo Optimizer

The optimal weighting factor of ANFIS is selected with the help of dingo optimizer. Dingos have a precise sense of correspondence. They talk to each other by detecting unique sound forces in the air. In DOX, dingo generates sound input so that dingo's can trade their intelligence with others to create normal local area nuances. Adequate amount of shaking can be changed through the strength of the individual as the dingo moves from one area to another [22].

Group hunting is an intriguing social behavior of dingos. Hunting practices are classified into their stages as follows:

- Chasing in addition approaching
- Encircling in addition harassing
- Attack

Encircling: Dingos can be capable of detecting the area of prey, following the area and following the alpha, circling the prey. To demonstrate dingo's social progressive structure, the current best professional approach is expected to be objective or point prey, which is best because the mission area is unknown. Meanwhile, other task systems are still trying to update their algorithms in the following imaginary algorithms.The behavior of dingos is shown by the accompanying numerical conditions (17) - (21).

$$\overrightarrow{D_d} = \left|\vec{A}.\overrightarrow{P_P}(X) - \vec{P}(i)\right| \qquad (17)$$

$$\vec{P}(i+1) = \overrightarrow{P_P}(X) - \vec{B}.\vec{D}(d) \qquad (18)$$

$$\vec{A} = 2.\overrightarrow{a_1} \qquad (19)$$

$$\vec{B} = 2\vec{b}.\overrightarrow{a_2} - \vec{b} \qquad (20)$$

$$\vec{b} = 3 - \left(1 * \left(\frac{3}{I_{max}}\right)\right) \qquad (21)$$

Positions of neighboring dingoes addressed using a two-tier level vector. As mentioned by the location of the prey $(P*, Q*)$,, a dingo (P, Q) can update its position in place. By changing the value of the vectors $\vec{A}$ and $\vec{B}$for the current area, each of the possible areas is arranged individually on the map around the best expert.

Table 1: Parameters of dingo optimizer

Elements	Description
I_{max}	Maximum number of iterations
$\vec{b}$	Linearly decreased from 3 to 0 at every iteration
$\overrightarrow{a_2}$	Random parameter in [0,1]
$\overrightarrow{a_1}$	Random parameter in [0,1]
$\vec{B}$	Coefficient vector
$\vec{A}$	Coefficient vector
$\vec{P}(i)$	Position vector (dingo)
$\overrightarrow{P_P}(X)$	Position vector (prey)
$\overrightarrow{D_d}$	Distance among the dingo and prey

It's useful to look at the optimism side by side [23-25]. Following the part of a dingo that arbitrarily maintains the value of the prey, it is important not to bend the dingo or encounter the past. Deliberately, we used $\vec{A}$ to give a random trial value from base to last importance. This strategy is possible in protecting the arrangement from nearby Optima. In the long run, DOX ends up at the point where it meets the final steps. Based on the dingo optimizer, the optimal weighting parameter is selected. Finally, the proposed methodology is utilized to control the DAB for managing the power flow in interconnected DC microgrid.

4. Outcome Evaluation

This section assesses the projected technique's presentation. MATLAB/System is used to implement the anticipated system simulation. Table 1 displays the planned system's simulation parameters. The intended system runs on an Intel Core i7 processor running at 4GHz and 32 GB. The intended converter is designed to control the DC microgrid system's load management. The proposed method is designed to control the microgrid system's power flow analysis. The electric grid system's load requirements are compensated for by using the entire projected controller.

Table 2: Implementation parameters

S. No	Components	Description	Value
1		Input voltage	100V
2	Boost converter	Resistance	1e-3 ohm
3		Inductor	250e-6H
4		Capacitance	200e-6F
5	Buck Converter	Resistance	0.02 ohm
6		Inductance	3e3H
7		Capacitance	30e-6F
8	PI controller	proportional constant	0.5785
9		Integral constant	0.0643
10		Nominal power	1000VA
11		Nominal frequency	50Hz
12		Capacitance	1e-6F
13		Resistance	1 ohm
14		Input voltage	100V
15		Resistance	1e-3 ohm
16		Inductor	250e-6H

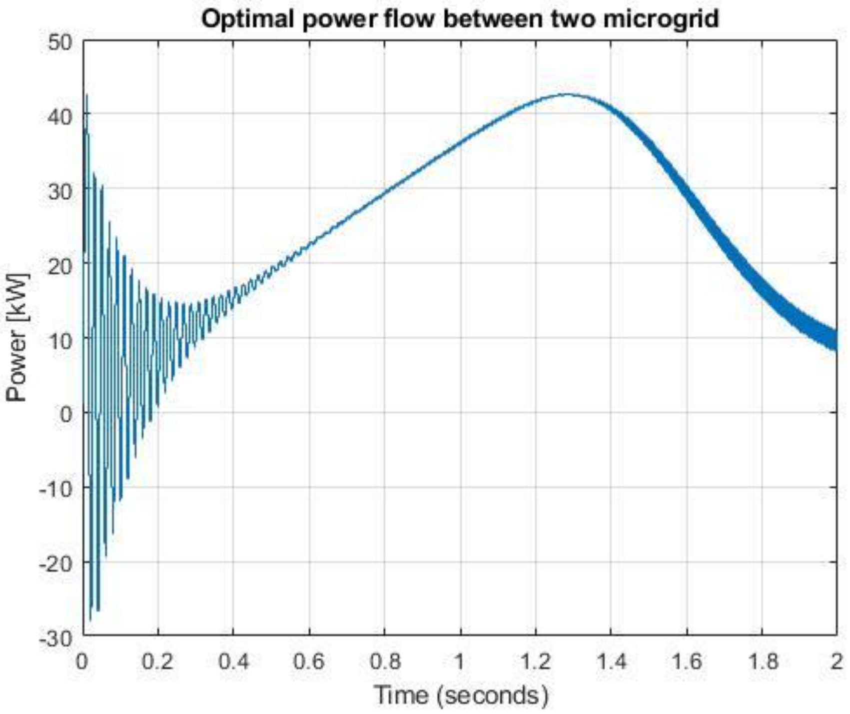

Figure 3: power flow analysis of the proposed controller

This suggested controller helps to improve the ideal power flow. The suggested controller improves the ideal power flow between the utility grid and DC microgrid. Figure 3 displays the suggested controller's power flow management. The dual active bridge converter and the suggested controller are used to control the power flow. The WOA and FFA, respectively, are compared with the suggested controller.

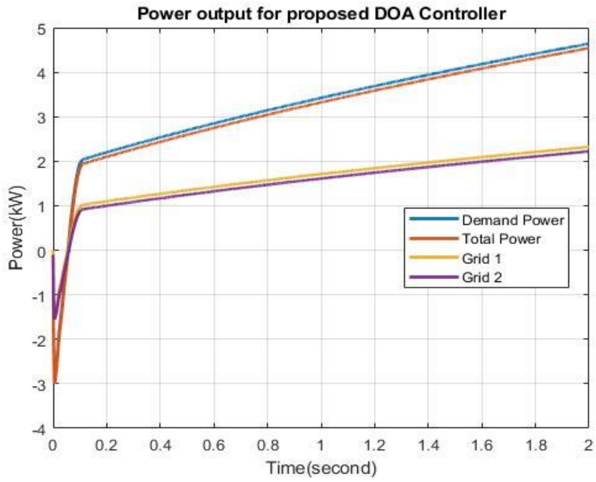

Figure 4: The output power output of proposed controller

The output power of the proposed controller is 2KW which illustrated in figure 4. The proposed controller is analyzed with demand power, total power, grid 1 and grid power. In figure 4, the demand power of the system: maximum is 5KW and minimum is 2KW. Additionally, the total power of the system is a similar of the demand power which is achieved with the assistance of the proposed controller and proposed converter. The grid 1 power is 1KW and grid 2 power is 1KW. Based on the analysis, the proposed controller is achieved efficient power output in the DC microgrid system. The grid 1 and grid 2 power requirements are achieved with the consideration of PV generation and BESS power.

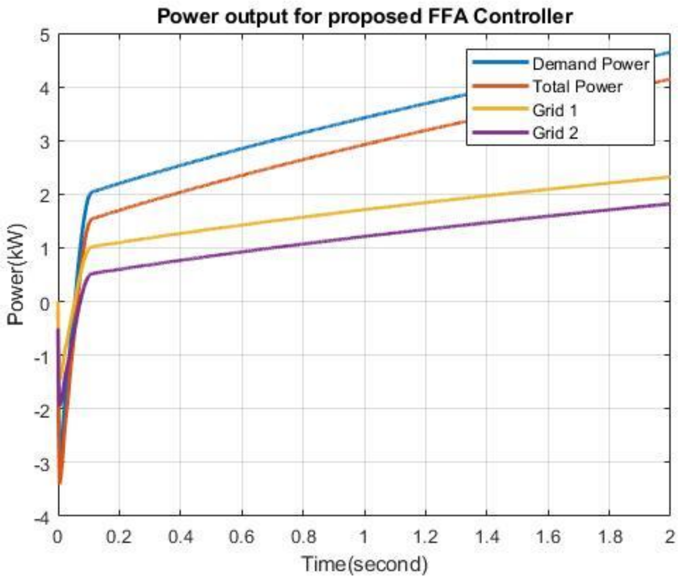

Figure 5: The output power output of proposed controller

The output power of the FFA controller is 2KW which illustrated in figure 5. The proposed controller is analyzed with demand power, total power, grid 1 and grid power. In figure 5, the demand power of the system: maximum is 5KW and minimum is 2KW. Additionally, the total power of the system is a similar of the demand power which is achieved with the assistance of the FFA controller and proposed converter. The grid 1 power is 1KW and grid 2 power is 1KW. Based on the analysis, the FFA controller is not achieved power output in the DC microgrid system. The grid 1 and grid 2 power requirements are failed to achieve with the consideration of PV generation and BESS power.

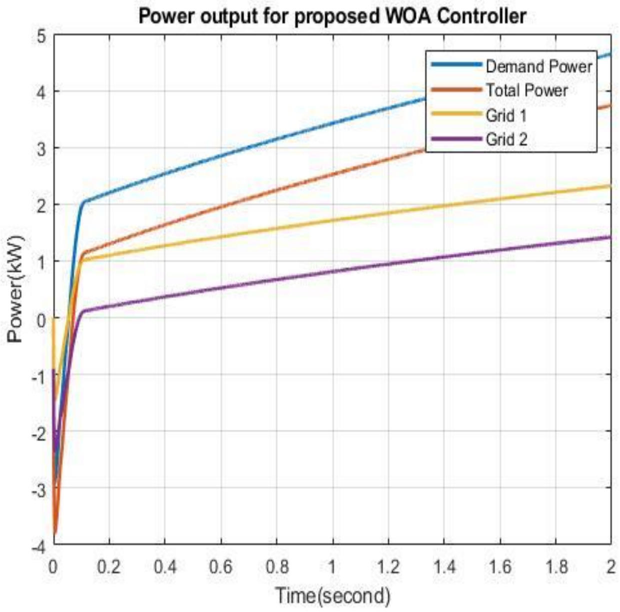

Figure 6: The output power output of WOA controller

The output power of the WOA controller is 2KW which illustrated in figure 6. The proposed controller is analyzed with demand power, total power, grid 1 and grid power. In figure 6, the demand power of the system: maximum is 5KW and minimum is 2KW. Additionally, the total power of the system is a similar of the demand power which is achieved with the assistance of the WOA controller and proposed converter. The grid 1 power is 1KW and grid 2 power is 1KW. Based on the analysis, the WOA controller is not achieved power output in the DC microgrid system. The grid 1 and grid 2 power requirements are failed to achieve with the consideration of PV generation and BESS power.

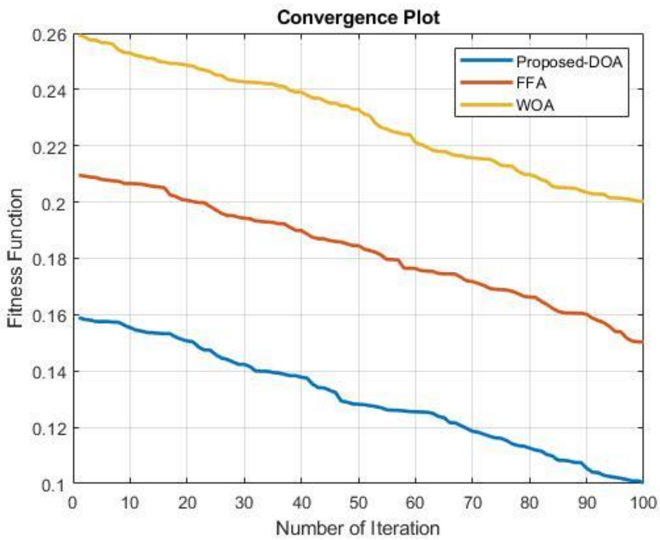

Figure 7: Convergence analysis

The proposed methodology is compared with the conventional techniques, such as FFA and WOA. The WOA is converged and achieved the 0.26 fitness function; similarly, the FFA is converged and achieved the 0.21 fitness function. The convergence analysis is a crucial plot to validate the proposed system. The suggested controller helps to reach the 0.16 fitness function convergence. The research reveals that the suggested controller achieves efficient convergence in terms of the fitness function.

5.Conclusion

In order to regulate the component output power and lessen the fluctuation between the generation and consumption of power while maintaining a steady DC bus voltage, IANFIS has been developed in this article. In order to maintain power balance in a stand-alone DC microgrid where DAB converters interfaced the RES and BES unit, this study proposes a power management control strategy.The generation side, or PV system and BES, is coupled to the storage systems and renewable energy sources. Furthermore, a DC microgrid is connected to the load demand. Through the use of twin active bridge converters, the generating and storage systems serve to balance the load demand. The DAB is connected with the dual DC microgrid system for managing power flow among the two DC microgrids. This dual active bridge converter is utilized to balance the power among Dual DC microgrids. In this suggested approach, the IANFIS is used to enhance the dual active bridge converter's performance. The IANFIS is a combination of ANFISand DO. Here, the microgrid components are indirectly or directly connected to this DC grid with the assistance of power electronic interfaces for connecting PV and BESS. The proposed methodology is developed to manage the power among generation and load demand management. The proposed method is evaluated on a dual active bridge converter connected microgrid system with the components of PV and BESS respectively. The suggested approach is contrasted with traditional techniques like FFA and WOA.

Compliance with Ethical Standards

Conflict of interest

The authors declare that they have no conflict of interest.

Human and Animal Rights

This article does not contain any studies with human or animal subjects performed by any of the authors.

Informed Consent

Informed consent does not apply as this was a retrospective review with no identifying patient information.

Funding: Not applicable

Conflicts of interest Statement: Not applicable

Consent to participate: Not applicable

Consent for publication: Not applicable

Availability of data and material:

Data sharing is not applicable to this article as no new data were created or analyzed in this study.

Code availability: Not applicable

References

[1]. Zolfaghari, M., Gharehpetian, G.B., Shafie-khah, M. and Catalão, J.P., 2022. Comprehensive review on the strategies for controlling the interconnection of AC and DC microgrids. International Journal of Electrical Power & Energy Systems, 136, p.107742.

[2]. Suman, G.K., Guerrero, J.M. and Roy, O.P., 2021. Robust Frequency Control in Interconnected Microgrids: An H $ _2 $/H $ _ {\infty} $ Control Approach. IEEE Systems Journal.

[3]. Ahmad, S., Mekhilef, S. and Mokhlis, H., 2021, September. An Intelligent Interconnection Module for Multiple Self-healed Interconnected Microgrids. In 2021 IEEE 4th International Conference on Computing, Power and Communication Technologies (GUCON) (pp. 1-6). IEEE.

[4]. Kumar, A. and Ghose, T., 2021. A Newton-Raphson-based unified load flow of grid-connected and islanded AC–DC microgrids. International Transactions on Electrical Energy Systems, 31(11), p.e13075.

[5]. Zargar, R.H.M. and Yaghmaee, M.H., 2021. Energy exchange cooperative model in SDN-based interconnected multi-microgrids. Sustainable Energy, Grids and Networks, 27, p.100491.

[6]. Samson, S.Y. and Chau, T.K., 2022. Pinning Decision in Interconnected Systems with Communication Disruptions under Multi-Agent Distributed Control Topology. International Journal of Robotics and Control Systems, 2(1), pp.18-36.

[7]. Vuyyuru, U., Maiti, S. and Chakraborty, C., 2019. Active power flow control between dc microgrids. IEEE Transactions on Smart Grid, 10(5), pp.5712-5723.

[8]. Zolfaghari, M., Gharehpetian, G.B., Shafie-khah, M. and Catalão, J.P., 2022. Comprehensive review on the strategies for controlling the interconnection of AC and DC microgrids. International Journal of Electrical Power & Energy Systems, 136, p.107742.

[9]. Vuyyuru, U., Maiti, S. and Chakraborty, C., 2019, October. Universal active power flow controller with common energy storage support for dc-microgrids. In IECON 2019-45th Annual Conference of the IEEE Industrial Electronics Society (Vol. 1, pp. 2518-2523). IEEE.

[10]. Han, Y., Pu, Y., Li, Q., Fu, W., Chen, W., You, Z. and Liu, H., 2019. Coordinated power control with virtual inertia for fuel cell-based DC microgrids cluster. International Journal of Hydrogen Energy, 44(46), pp.25207-25220.

[11]. Li, Q., Li, A., Wang, T. and Cai, Y., 2021. Interconnected hybrid AC-DC microgrids security enhancement using blockchain technology considering uncertainty. International Journal of Electrical Power & Energy Systems, 133, p.107324.

[12]. Zolfaghari, M., Abedi, M. and Gharehpetian, G.B., 2019. Power flow control of interconnected AC–DC microgrids in grid-connected hybrid microgrids using modified UIPC. IEEE Transactions on Smart Grid, 10(6), pp.6298-6307.

[13]. Li, F., Qin, J., Wan, Y. and Yang, T., 2020. Decentralized cooperative optimal power flow of multiple interconnected microgrids via negotiation. IEEE Transactions on Smart Grid, 11(5), pp.3827-3836.

[14]. Zolfaghari, M., Abedi, M. and Gharehpetian, G.B., 2019, June. Power exchange control of clusters of multiple AC and DC microgrids interconnected by UIPC in hybrid microgrids. In 2019 24th Electrical Power Distribution Conference (EPDC) (pp. 22-26). IEEE.

[15]. Panda, M., Bhaskar, D.V. and Maity, T., 2022. An efficient SoC-balancing based power management strategy for interconnected subgrids of DC microgrid. Journal of Energy Storage, 50, p.104287.

[16]. Datta, Amit Jyoti, Arindam Ghosh, Firuz Zare, and Sumedha Rajakaruna. "Bidirectional power sharing in an ac/dc system with a dual active bridge converter." IET Generation, Transmission & Distribution 13, no. 4 (2019): 495-501.

[17]. Jacob, Ammu Susanna, Rangan Banerjee, and Prakash C. Ghosh. "Sizing of hybrid energy storage system for a PV based microgrid through design space approach." Applied energy 212 (2018): 640-653.

[18]. Thiyagu Arunkumari, Vairavasundaram Indragandhi, Gopal Arunkumar, Padmanaban Sanjeevikumar, and Jens Bo Holm-Nielsen, "Implementation of high-gain nonisolated DC-DC converter for PV-fed applications", An International Transactions on Electrical Energy Systems, Vol.30, No.1, 2020.

[19]. AlRassas, Ayman Mutahar, Mohammed AA Al-qaness, Ahmed A. Ewees, Shaoran Ren, Mohamed Abd Elaziz, Robertas Damaševičius, and Tomas Krilavičius. "Optimized ANFIS model using Aquila Optimizer for oil production forecasting." Processes 9, no. 7 (2021): 1194.

[20]. Sowinski, Janusz. "The Impact of the Selection of Exogenous Variables in the ANFIS Model on the Results of the Daily Load Forecast in the Power Company." Energies 14, no. 2 (2021): 345.

[21]. Olayode, Isaac Oyeyemi, Alessandro Severino, Lagouge Kwanda Tartibu, Fabio Arena, and Ziya Cakici. "Performance Evaluation of a Hybrid PSO Enhanced ANFIS Model in Prediction of Traffic Flow of Vehicles on Freeways: Traffic Data Evidence from South Africa." Infrastructures 7, no. 1 (2021): 2.

[22]. Bairwa, Amit Kumar, Sandeep Joshi, and Dilbag Singh. "Dingo Optimizer: A Nature-Inspired Metaheuristic Approach for Engineering Problems." Mathematical Problems in Engineering 2021 (2021).

[23]. Almazán-Covarrubias, Juan H., Hernán Peraza-Vázquez, Adrián F. Peña-Delgado, and Pedro Martín García-Vite. "An Improved Dingo Optimization Algorithm Applied to SHE-PWM Modulation Strategy." Applied Sciences 12, no. 3 (2022): 992.

[24]. Singh, Beant, Parag Nijhawan, Manish Kumar Singla, Jyoti Gupta, and Parminder Singh. "Hybrid algorithm for parameter estimation of fuel cell." International Journal of Energy Research (2022).

[25]. Peraza-Vázquez, Hernán, Adrián F. Peña-Delgado, Gustavo Echavarría-Castillo, Ana Beatriz Morales-Cepeda, Jonás Velasco-Álvarez, and Fernando Ruiz-Perez. "A bio-inspired method for engineering design optimization inspired by dingoes hunting strategies." Mathematical Problems in Engineering 2021 (2021).